

Analytic expression for the proton structure function in deep inelastic scattering^{*}

XIANG Wen-Chang(向文昌) ZHOU Dai-Cui(周代翠)¹⁾

WAN Ren-Zhuo(万仁卓) YUAN Xian-Bao(袁显宝)

(Institute of Particle Physics, Huazhong Normal University;
The Key Laboratory of Quark and Lepton Physics (Huazhong Normal University),
Ministry of Education, Wuhan 430079, China)

Abstract The analytic expression of proton in deep inelastic scattering is studied by using the color glass condensate model and the dipole picture. We get a better description of the HERA DIS data than the GBW model which was inspired by the Glauber model. We find that our model satisfies the unitarity limit and Froissart Bound which refers to an energy dependence of the total cross-section rising no more rapidly than $\ln^2 s$.

Key words deep inelastic scattering, color glass condensate, proton structure function

PACS 14.20.Dh, 13.85.Hd, 11.55.Bq

1 Introduction

The problem of understanding the large gluon density regime in high energy scattering has always been one of the challenges of perturbative QCD. Unitarity of the total cross-section and saturation of the gluon distribution are among the most important issues related to the problem. The high energy or small Bjorken x regime of deep inelastic lepton-hadron scattering (DIS) at HERA provides a good opportunity to study the parton saturation physics. A first hint towards saturation effects at HERA came from the success of the simple “saturation model” by Golec-Biernat and Wuesthoff (GBW)^[1] which provided a reasonable description of the proton structure function at HERA for $x \leq 10^{-2}$ and all Q^2 . This model has been implemented within the color dipole picture which is also the framework for the present analysis. The dipole picture is a factorization scheme for DIS, which is valid at small x and is particularly convenient for the inclusion of unitarity corrections. Specifically, the scattering between the virtual photon γ^* and the proton is seen as the dissociation of γ^* into a quark-

antiquark color dipole pair followed by the interaction of this dipole with the color fields in the proton. The most important thing for us is the fact that the mechanism leading to the dissociation of the photon and the subsequent scattering can be factorized and written in terms of a photon wave function convoluted with a quark-antiquark cross section $\hat{\sigma}_{\text{dipole}}$. This leads to the following expressions for the γ^*p cross-sections and the F_2 structure function^[2]:

$$\sigma_{T,L}(x, Q^2) = \int d^2\mathbf{r} \int_0^1 dz |\psi_{T,L}(z, \mathbf{r})|^2 \hat{\sigma}_{\text{dipole}}(x, r^2), \quad (1)$$

$$F_2(x, Q^2) = \frac{Q^2}{4\pi^2\alpha_{\text{em}}} (\sigma_T + \sigma_L). \quad (2)$$

and

$$|\Psi_T^{(f)}(z, \mathbf{r}, \mathbf{r}'; Q^2)|^2 = \frac{\alpha_{\text{em}} N_c}{2\pi^2} e_f^2 \left((z^2 + (1-z)^2) \times \right. \\ \left. \varepsilon_f^2 \frac{\mathbf{r} \cdot \mathbf{r}'}{|\mathbf{r}| |\mathbf{r}'|} K_1(\varepsilon_f |\mathbf{r}|) K_1(\varepsilon_f |\mathbf{r}'|) + \right. \\ \left. m_f^2 K_0(\varepsilon_f |\mathbf{r}|) K_0(\varepsilon_f |\mathbf{r}'|) \right), \quad (3)$$

Received 22 April 2008, Revised 28 July 2008

^{*} Supported by NSFC (10875051, 10575044, 10635020), Chinese Ministry of Education (306022, IRT 0624) and State Key Development Program of Basic Research of China (2008CB317106)

1) E-mail: dczhou@mail.ccnu.edu.cn

©2009 Chinese Physical Society and the Institute of High Energy Physics of the Chinese Academy of Sciences and the Institute of Modern Physics of the Chinese Academy of Sciences and IOP Publishing Ltd

$$|\Psi_L^{(f)}(z, \mathbf{r}, \mathbf{r}'; Q^2)|^2 = \frac{\alpha_{\text{em}}^2 N_c}{2\pi^2} e_f^2 4Q^2 z^2 (1-z)^2 \times \\ K_0(\varepsilon_f |\mathbf{r}|) K_0(\varepsilon_f |\mathbf{r}'|). \quad (4)$$

Here, $\psi_{T,L}$ are the light-cone wave functions for γ^* with transverse or longitudinal polarization, which can be computed with QED. σ_{dipole} is the cross-section for a dipole with transverse size \mathbf{r} scattering off a proton and encodes all the information about the hadronic interactions, like unitarization effects. The e_f and m_f are the charge and mass of the quark with flavor f and

$$\varepsilon_f^2 = z(1-z)Q^2 + m_f^2. \quad (5)$$

The analytic study of the proton structure function has absorbed a lot of interest in Refs. [3, 4]. Based on the Froissart Bound^[5], which refers to an energy dependence of the total cross-section rising no more rapidly than $\ln^2 s$, they proposed an analytic expression for the joint x and Q^2 dependences of the proton structure function in deep inelastic scattering. However, they neglected the fact that the gluons inside the high energy parton will form a new matter called color glass condensate which plays an important role in the calculation of the parton structure function at small x and high energy. In this paper, we use the color glass condensate model and the dipole picture to compute the proton structure function in DIS and get an analytic expression of the proton structure function, and we will show that this expression satisfies the Froissart Bound automatically.

2 Dipole cross-section

To calculate the total cross-section of γ^*p scattering we should know the dipole cross-section σ_{dipole} which includes all the information about the quark-antiquark dipole scattering off the target proton. In our analysis we take for σ_{dipole} the GWB model which has been modelled as^[1, 2]:

$$\sigma_{\text{dipole}}(x, r) = \sigma_0 \left(1 - e^{-\frac{r^2 Q_s^2(x)}{4}} \right), \quad (6)$$

where $Q_s^2(x)$ plays the role of the saturation momentum which is a measure of the gluon density in the impact parameter space and parametrized as:

$$Q_s^2(x) = 1 \text{ GeV}^2 \cdot \left(\frac{x_0}{x} \right)^\lambda. \quad (7)$$

This choice is motivated by the following considerations,

1) $rQ_s(x)/2 \geq 1$, this happens when the proton starts to look dark. Such a microscopic interpretation is no more valid but the exponential has the virtue to

force the cross section to tend towards a constant at large $rQ_s(x)$, thus respecting the unitarity constraint through a strict compliance with the Froissart bound.

2) $rQ_s(x)/2 \sim 1$, the exponential in Eq. (6) takes care of resumming many gluon exchanges, in a Glauber-inspired way.

3) $rQ_s/2 \leq 1$, the model reduces to color transparency.

In Eq. (6) the saturation is visible by the fact that the dipole scattering amplitude $N(x, \mathbf{r}) = 1 - e^{-r^2 Q_s^2(x)/4}$ approaches the unitarity bound $N = 1$ for a dipole size larger than a characteristic size $1/Q_s(x)$, which decreases when decreasing x . By fitting the three parameters σ_0 , x_0 and λ , GBW manages to give a rather good description of the HERA data, for both the inclusive and the diffractive structure functions.

In order to compute the analytic proton structure function in the following study, we apply the Mellin transformation to the dipole cross-section (6) and obtain^[1]:

$$G(\nu) = \int_0^\infty d\hat{r} (\hat{r}^2)^{-3/2-i\nu} (1 - e^{-\hat{r}^2}) = -\Gamma\left(-\frac{1}{2} - i\nu\right) \quad (8)$$

with $\hat{r} = rQ_s(x)/2$.

3 Proton structure function in deep inelastic scattering

To obtain the analytic expression for the proton structure function in deep inelastic scattering, we use the color glass condensate model and the dipole picture to calculate the total γ^*p cross-section. In the dipole picture one can use the Mellin transformation to factorize the wave function in Eq. (1) and gets^[1]:

$$\sigma_{T,L}(x, Q^2) = \int \frac{d\nu}{2\pi} \int d^2\mathbf{r} \int_0^1 dz |\psi_{T,L}(z, \mathbf{r})|^2 \times \\ \int \frac{d\mathbf{r}'^2}{r'^2} \left(\frac{r}{r'} \right)^{1+2i\nu} \sigma(x', r'^2) = \\ \sigma_0 \int \frac{d\nu}{2\pi} \left[\left(\frac{x_0}{x'} \right)^\lambda \frac{Q_0^2}{Q^2} \right] H_{T,L} \left(\nu, \frac{m_f^2}{Q^2} \right) G(\nu). \quad (9)$$

To simplify the computation, we set $m_f = 0$ in this paper. $H_{T,L}(\nu, 0)$ has the form

$$H_T(\nu, 0) = \sum_f e_f^2 \frac{6\alpha_{\text{em}}}{2\pi} \frac{\pi}{16} \frac{9/4 + \nu^2}{1 + \nu^2} \left(\frac{\pi}{\cos(\pi\nu)} \right)^2 \times \\ \frac{\sinh(\pi\nu)}{\pi\nu} \frac{\Gamma(3/2 + i\nu)}{-\Gamma(-1/2 - i\nu)} \quad (10)$$

and

$$H_L(\nu, 0) = \sum_f e_f^2 \frac{6\alpha_{\text{em}}}{2\pi} \frac{\pi}{8} \frac{1/4 + \nu^2}{1 + \nu^2} \left(\frac{\pi}{\cos(\pi\nu)} \right)^2 \times \frac{\sinh(\pi\nu)}{\pi\nu} \frac{\Gamma(3/2 + i\nu)}{-\Gamma(-1/2 - i\nu)}. \quad (11)$$

Let's look at the analytical structure of the cross-section (9) in the complex ν -plane. The integration over ν goes along the real axis and one can close the contour in the upper or lower part of the complex plane. In the hard regime where Q^2 is very large, the argument $(x_0/x)^\lambda Q_0^2/Q^2$ is less than 1, one closes the contour in the lower plane. To leading order the integration over ν in the lower complex plane, enclosing the double pole at $\nu = -i/2$ leads to the logarithmic behavior of the cross-section^[1]:

$$\left(\frac{x_0}{x} \right)^\lambda \frac{Q_0^2}{Q^2} \ln \left[\left(\frac{x}{x_0} \right)^\lambda \frac{Q^2}{Q_0^2} \right]. \quad (12)$$

In the soft regime where Q^2 is small, the argument $(x_0/x)^\lambda Q_0^2/Q^2$ is larger than 1, we close the contour in the upper plane. To leading order the integration over ν in the upper complex plane, enclosing the double pole at $\nu = i/2$ gives the following logarithmic behavior of the cross-section^[1]:

$$\ln \left[\left(\frac{x_0}{x} \right)^\lambda \frac{Q_0^2}{Q^2} \right]. \quad (13)$$

Combining the hard and soft terms, one gets the analytical expression of the total γ^*p scattering cross-section:

$$\sigma^{\gamma^*p}(x, Q^2) = \sigma'_0 \left\{ \ln \left[\left(\frac{x'_0}{x} \right)^{\lambda'} \frac{Q_0^2}{Q^2} + 1 \right] + \left(\frac{x'_0}{x} \right)^{\lambda'} \frac{Q_0^2}{Q^2} \ln \left[\left(\frac{x}{x'_0} \right)^{\lambda'} \frac{Q^2}{Q_0^2} + 1 \right] \right\}, \quad (14)$$

where the 1 in the argument of the logarithms assures the matching of the transition between the hard and soft regime. Note that the total γ^*p scattering cross-section grows with energy slower than $\ln^2 s$ ($\ln(1/x) \propto \ln s$), which indicates that the total cross-section satisfies the Froissart Bound. Finally, we get the analytical expression of the proton structure function in deep inelastic scattering by using the relation between the total γ^*p scattering cross-section σ^{γ^*p}

and the parton structure function F_2 ,

$$F_2(x, Q^2) = \frac{Q^2}{4\pi^2\alpha_{\text{em}}} \sigma^{\gamma^*p}(x, Q^2) = \frac{Q^2}{4\pi^2\alpha_{\text{em}}} \sigma'_0 \left\{ \ln \left[\left(\frac{x'_0}{x} \right)^{\lambda'} \frac{Q_0^2}{Q^2} + 1 \right] + \left(\frac{x'_0}{x} \right)^{\lambda'} \frac{Q_0^2}{Q^2} \ln \left[\left(\frac{x}{x'_0} \right)^{\lambda'} \frac{Q^2}{Q_0^2} + 1 \right] \right\}, \quad (15)$$

with $Q_0^2 = 1 \text{ GeV}^2$, where the three parameters σ'_0 , x_0 and λ are determined by a fit to the F_2 data.

4 Numerical study the proton structure function

To determine the parameters of the proton structure function (15), we fitted the ZEUS data for the F_2 structure function in the kinematical range $x \leq 10^{-2}$ and $0.045 \text{ GeV}^2 < Q^2 < 50 \text{ GeV}^2$. The upper limit on Q^2 has been chosen large enough to include a large amount of ‘‘perturbative’’ data points, but low enough in order to justify the use of the BFKL dynamics, rather than the DGLAP evolution. We have considered only the ZEUS data^[6–8] because there is a mismatch between the H1 and ZEUS data regarding the data normalization and since only ZEUS has data also in the low Q^2 region, i.e., in the saturation region. To fix the parameters we minimize $\chi^2 = \sum_i (\text{model}(i, p_1, \dots, p_n) - F_2(i))^2 / (\text{error}(i))^2$, where the sum goes over the data points, p_1, \dots, p_n denote the parameters to be found, $F_2(i)$ the experimental results for the F_2 structure function, and for the error of F_2 , i.e., $(\text{error}(i))^2$, we use the systematic error squared plus the statistical error squared^[9].

Table 1 gives the parameters which come from the fit of the F_2 data by using GBW and our model. Our model leads to a relatively much better description of the HERA data, as can be seen from the comparison of the χ^2 values and the two lines in the Fig. 1.

Table 1. The parameters of the GBW and of the our structure function.

model/ parameters	χ^2	$\chi^2/\text{d.o.f}$	$x_0 (\times 10^{-2})$	λ	R/fm
F_2^{GBW}	266.22	1.74	0.0411	0.285	0.594
F_2	150.36	0.986	0.146	0.328	0.712

By using the parameters in Table 1, we obtain the final analytic expression of proton structure function in deep inelastic scattering

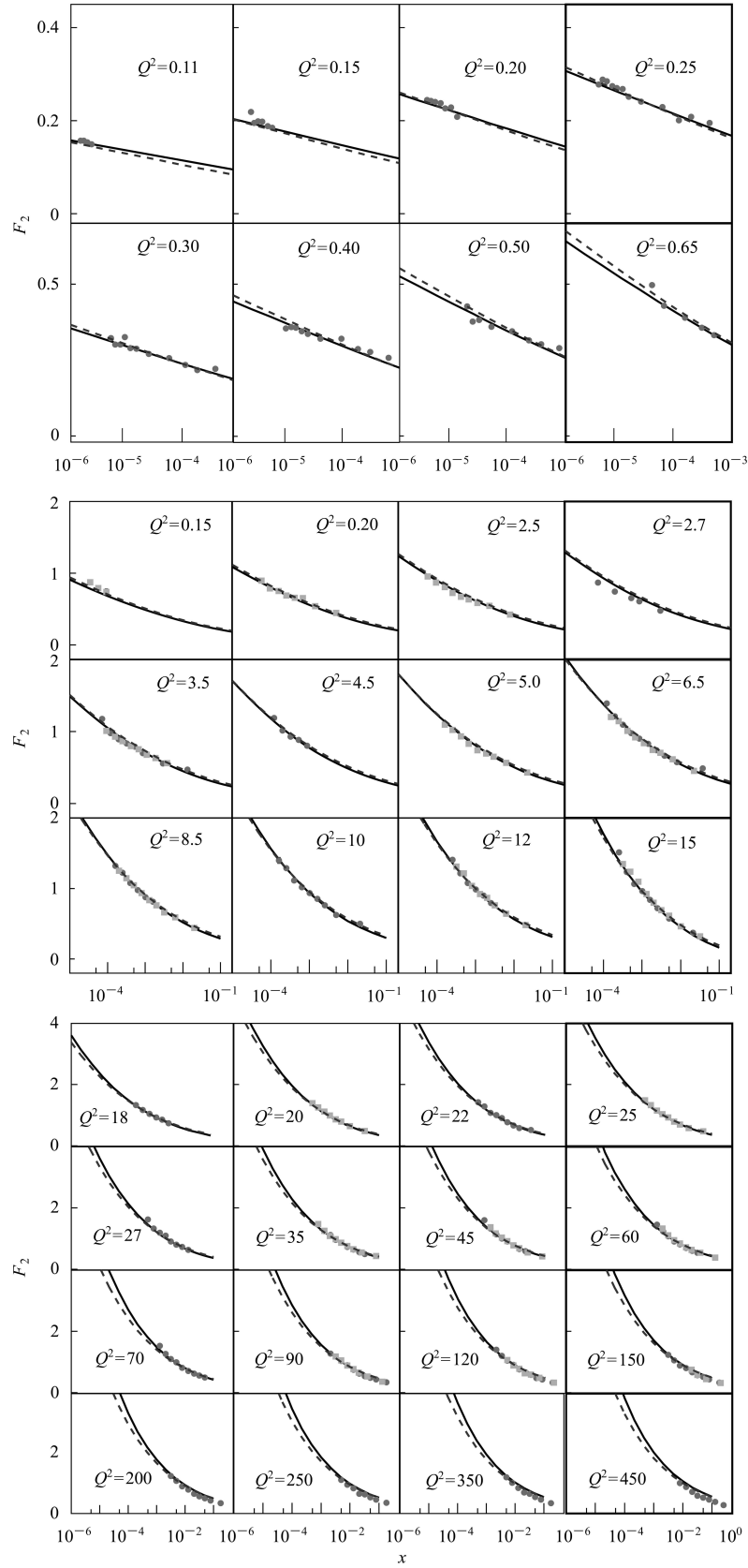


Fig. 1. The F_2 structure function versus x at different values of Q^2 . The experimental points are the latest published data from the H1 (squares) and ZEUS (dots) collaborations^[6–8]. The solid line represents the result of analytical F_2 structure function and the dashed line the result of the GBW fit to the ZEUS data for $x \leq 10^{-2}$ and $0.45\text{GeV}^2 < Q^2 < 50\text{ GeV}^2$. The data points at lowest Q^2 values, 0.045, 0.065 and 0.085 GeV^2 , are not shown here although they are included in the fits.

$$\begin{aligned}
F_2(x, Q^2) = & \\
& 0.256Q^2 \left\{ \ln \left[\left(\frac{0.146 \times 10^{-2}}{x} \right)^{0.328} \frac{Q_0^2}{Q^2} + 1 \right] + \right. \\
& \left. \left(\frac{0.146 \times 10^{-2}}{x} \right)^{0.328} \frac{Q_0^2}{Q^2} \times \right. \\
& \left. \ln \left[\left(\frac{x}{0.146 \times 10^{-2}} \right)^{0.328} \frac{Q^2}{Q_0^2} + 1 \right] \right\}, \quad (16)
\end{aligned}$$

with $Q_0^2 = 1 \text{ GeV}^2$.

5 Conclusions

In this paper, we use the color glass condensate

model and the dipole picture to calculate the total cross-section of γ^*p scattering and get an analytic expression for the proton structure function in deep inelastic scattering. We wish to note that our model leads to a relatively much better description of the HERA data, as can be seen from the comparison of the χ^2 values in Table 1. The total γ^*p scattering cross-section grows up with the energy slower than $\ln^2 s$ ($\ln(1/x) \propto \ln s$) in Eq. (14), which indicates that the total cross-section satisfies the Froissart Bound.

We will present the generalization of this approach to compute the gluon distribution function $G(x, Q^2) = xg(x, Q^2)$ in leading order directly from a global parametrization of the data on $F_2^p(x, Q^2)$ in our next work.

References

- 1 Golec-Biernat K J, Wusthoff M. Phys. Rev. D, 1999, **59**: 014017
- 2 Golec-Biernat K J, Wusthoff M. Phys. Rev. D, 1999, **60**: 114023
- 3 Berger E L, Block M M, Chung-I Tan. Phys. Rev. Lett., 2007, **98**: 242001
- 4 Block M M, Berger E L, Chung-I Tan. Phys. Rev. Lett., 2006, **97**: 252003
- 5 Froissart M. Phys. Rev., 1961, **123**: 1053
- 6 Breitweg J et al. (ZEUS Collaboration). Phys. Lett. B, 2000, **487**: 53
- 7 Chekanov S et al. (ZEUS Collaboration). Eur. Phys. J. C, 2001, **21**: 443
- 8 Adloff C et al. (H1 Collaboration). Eur. Phys. J. C, 2001, **21**: 33
- 9 Kozlov M, Shoshi A, XIANG W. JHEP, 2007, **10**: 20